Electronic Spectroscopy in Condensed Media. Monte-Carlo Simulation of Spectral Properties of the Aqueous Nitrite Ion

Ajit Banerjee and Jack Simons*†

Contribution from the Department of Chemistry, University of Utah, Salt Lake City, Utah 84112. *Received July 22, 1980*

Abstract: Monte-Carlo simulation of the hydration structure and the spectroscopic quantities (excitation energy, and inhomogeneous broadening) for the $n\pi^*$ electronic transition of the aqueous nitrite ion is presented. The structure of NO_2^-–$(H_2O)_n$ clusters is dominated by the strong (~27 kcal/mol) anisotropic NO_2^-–H_2O potential leading to preferential population of water molecules around the nitrite ion. The second hydration layer is seen to begin to form before the inner layer is complete. The calculated aqueous-phase excitation ($0 \rightarrow 0$) energy when compared to the gas-phase value shows a significant differential stabilization (~0.43 eV) of the excited ($^1B_1$) electronic state relative to the ground ($^1A_1$) state of the NO_2^- ion. The quadratic and cubic fluctuations of the excitation energy which constitute the inhomogeneous broadening of each vibrational line are calculated. It is found that the effects of the cubic fluctuations in the excitation-energy distribution may not be entirely negligible.

I. Introduction

In the research described in the present manuscript, our aim has been to analyze the effects of solvation on electronic spectra in terms of solute–solvent interactions. Recently, we developed a formalism for treating the spectroscopy and mobility of electrons, anions, and charge-transfer complexes in pure and mixed solvents within the statistical mechanical framework of time-correlation functions.[1,2] In this theory, which is described in ref 1 (hereafter referred to as paper 1), the effects of the solvent are incorporated into an effective potential-energy function which modifies the solute's properties. This potential contains the equilibrium-averaged effects of the solute–solvent interactions as well as a time-dependent part arising from fluctuations in the solvent molecules' coordinates about their equilibrium values. In treating the electronic absorption spectrum, the application of the above-mentioned formalism leads to an expression for the absorption intensity which, in lowest order, contains information about the electronic–vibrational energy differences, transition dipole matrix elements, and Franck–Condon (FC) factors of the solute species as modified by the equilibrium-averaged field of the solvent. In addition, each of the vibrational transition lines is broadened by an amount σ, called the inhomogeneous broadening, arising from fluctuations in the solute's electronic energy levels caused by fluctuations in the solvent's instantaneous positions and orientations. The solvent's distribution function $\rho(\vec{R},\vec{0})$ around a solute species at the coordinate origin ($\vec{0}$) enters into determining σ. Higher order terms in our expression for the line shape involve contributions from the equilibrium-averaged intermolecular couplings between the electronic levels of the neighboring molecules as well as fluctuations in these coupling interactions. These higher order terms are, of course, only important in cases when electronic energy levels of the solute and solvent molecules couple strongly. They can be safely neglected, as is shown below by our ab initio analysis of the interactions between NO_2^- and H_2O, for the system being studied here.

Our theory has already been applied[2] to analyzing experimental spectra of numerous solvated ions and charge-transfer systems and has yielded valuable new information regarding the strengths of solute–solvent interactions. The work discussed in the present article is directed toward simulating certain equilibrium-averaged spectroscopic quantities (excitation energies and inhomogeneous broadening) by making use of ab initio quantum chemical methods in conjunction with Monte-Carlo simulation techniques. We have chosen to perform such a benchmark study on the aqueous nitrite ion (for which ample experimental information[3-6] is available) to attempt to either verify or refute the results of applying our earlier line shape analysis theory[1,2] to this same system. It is our belief that by studying one species from both the empirical point of view (i.e., extracting inhomogeneous broadening and other information from given experimental data as in paper 1) and the ab initio simulation point of view, we should derive maximum information about the strengths and weaknesses of our earlier theory.

In an earlier article[7] (henceforth referred to as paper II), we studied the equilibrium structure of small hydrate clusters NO_2^-–$(H_2O)_n$, $n = 1, \ldots 15$, by using Monte-Carlo techniques and a restricted Hartree–Fock (RHF)-level description of the ground-state NO_2^-–H_2O dimer interaction potential. In the present article we are concerned with spectral quantities associated with $^1A_1 \rightarrow {}^1B_1$ ($n \rightarrow \pi^*$) transition of the aqueous nitrite ion. The $^1A_1$ ground state of NO_2^- is known to lie about 2.4 eV below the ground state of NO_2 as a result of gas-phase laser photodetachment work of Herbst et al.[3] The first excited $^1B_1$ state of gaseous NO_2^-, which lies approximately 3.1 eV above its ground state, is hence autodetaching in character. However, in aqueous solution our calculations[8] show that the anion's states become stabilized to such an extent that this first excited $^1B_1$ state lies below the neutral molecule's (NO_2) ground state. Strickler and Kasha[4] studied the optical absorption spectra of the nitrite ion in aqueous solution at room temperature and assigned the lowest energy band at 28 200 cm^{-1} (3.5 eV) to the $^1A_1 \rightarrow {}^1B_1$ ($n \rightarrow \pi^*$) transition. They found this band to be structureless and to have a half-width of about 0.5 eV. Kebarle et al.[5] and Castleman et al.[6] have studied the structure and solvation energies of such small hydrate clusters of NO_2^-–$(H_2O)_n$ by using high-pressure mass spectrometry. From their work, we have information available concerning the differential enthalpies of hydration of $NO_2^-(H_2O)_n$. The relationship of these experimental investigations to the present work will be elaborated upon below.

In this article we reinvestigate some of the questions addressed in paper 2 by using a more sophisticated NO_2^-–H_2O interaction

† Camille and Henry Dreyfus Fellow; John S. Guggenheim Fellow.

(1) A. Banerjee and J. Simons, *J. Chem. Phys.*, **68**, 415 (1979).
(2) (a) J. McHale, A. Banerjee, and J. Simons, *J. Chem. Phys.*, **69**, 1406 (1978); (b) A. Banerjee and J. Simons, *ibid.*, **69**, 5538 (1978); (c) J. McHale and J. Simons, *ibid.*, **72**, 425 (1980); (d) J. McHale and J. Simons, *ibid.*, **67**, 389 (1977).
(3) E. Herbst, T. A. Patterson, and W. C. Lineberger, *J. Chem. Phys.*, **61**, 1300 (1974).
(4) S. J. Strickler and M. Kaha, *J. Am. Chem. Soc.*, **85**, 2899 (1963).
(5) N. Lee, R. G. Keesee, and A. W. Castleman, Jr., *J. Chem. Phys.*, **72**, 1089 (1980). A. W. Castleman, Jr., *Adv. Colloid Interface Sci.*, **10**, 73–128 (1979).
(6) J. D. Payzant, R. Yamdagni, and P. Kebarle, *Can. J. Chem.*, **49**, 3308 (1971); P. Kebarle, *Mod. Aspects Electrochem.*, **9**, 1 (1974).
(7) A. Banerjee, R. Shepard, and J. Simons, *J. Chem. Phys.*, in press.
(8) A. Banerjee and J. Simons, *J. Chem. Phys.*, **71**, 60 (1979).

0002-7863/81/1503-2180$01.25/0

potential, and we attempt to simulate the equilibrium-averaged excitation energy corresponding to the $0 \rightarrow 0$ vibrational transition (the band origin) as well as the second- and third-order fluctuations in this excitation energy. The second-order energy fluctuation gives rise to a (Gaussian) inhomogeneous broadening, whereas the third-order fluctuation gives an estimate of how skewed the excitation-energy distribution is. The method which we have adopted can be briefly summarized as follows. The aqueous nitrite ion is simulated by successively larger clusters of water molecules surrounding a nitrite ion: $NO_2^-(H_2O)_n$. The cluster size n is taken to be large enough to guarantee that the equilibrium-averaged excitation energy and inhomogeneous broadening are stable (nonvarying). The ground- and excited-electronic states of the clusters are calculated by using, within a pairwise additive energy approximation, the results of ab initio configuration–interaction (CI) calculations on the NO_2^-–H_2O dimer and Clementi's[9] H_2O–H_2O CI dimer potential. Monte-Carlo techniques are then used both to simulate the equilibrium spatial distributions of the solvent molecules in the presence of a ground-state NO_2^- ion and to permit the computation of the equilibrium-averaged excitation energy and its fluctuations. By employing the excited-state $NO_2^-(n\pi^*)$–H_2O interaction potential to compute the equilibrium distribution of the solvent molecules around $NO_2^-(n\pi^*)$, we could, of course, simulate the electronic fluorescence spectrum of NO_2^-. We have not carried out this straightforward simulation because of the absence of experimental derivatives of such fluorescence in NO_2^-(aq). In the next section of this paper, we discuss the CI procedure used to obtain the NO_2^-–H_2O interaction and present a brief analysis of the resulting intermolecular potential. In section III we discuss the results of our Monte-Carlo simulations of the solvent structure around NO_2^- as well as the distribution of electornic excitation energies. In section IV these results are summarized and our concluding remarks are made.

II. Calculation of the Ground and ($n\pi^*$) Excited States of $NO_2^-(H_2O)_n$

The energies of the ground and excited electronic states of $NO_2^-(H_2O)_n$ when partitioned into one-body, two-body, etc., interactions have the form

$$E^0(NO_2^-(H_2O)_n) = (E^0_{NO_2^-} + \sum_i^n E_i) + (\sum_i^n E^0_{NO_2^-,i} + \sum_{i<j} E_{ij}) + (\sum_{i<j} E^0_{NO_2^-,ij} + \sum_{i<j<k} E_{ijk}) + \ldots \quad (1)$$

and

$$E^*(NO_2^-(H_2O)_n) = (E^*_{NO_2^-} + \sum_i^n E_i) + (\sum_i^n E^*_{NO_2^-,i} + \sum_{i<j} E_{ij}) + (\sum_{i<j} E^*_{NO_2^-,ij} + \sum_{i<j<k} E_{ijk}) + \ldots \quad (2)$$

Here, $E^0_{NO_2^-}$ and $E^*_{NO_2^-}$ represent the ground- and excited-state energies of the isolated NO_2^- ion. $E^0_{NO_2^-,i}$ and $E^*_{NO_2^-,i}$ refer to the interaction energies of the ith water molecule with the ground- or excited-state anion, E_i represents the energy of the ith isolated water solvent molecule, and E_{ij} represents the pair interaction between solvent molecules i and j. In writing these expressions we assume that the solvent water molecules are unchanged when the system is electronically excited, which permits us to use the same pair potential (E_{ij}) in the ground- and excited-state energy expressions. This is, of course, an assumption whose validity is strongly supported by our observations (see below) that the $n\pi^*$ excitation event is highly localized on the NO_2^- ion for thermally accessible geometries. Clementi[9] and others have found that three-body (and higher) interactions are generally small ($\sim$10% of the hydration energy) for ion–water systems. Therefore, we choose to approximate the cluster interaction energies by retaining only the pairwise interactions in eq 1 and 2. We give below additional justifications based on an analysis of the physical nature of the NO_2^-–H_2O interaction, for neglecting three- and higher-body interactions in computing cluster energies.

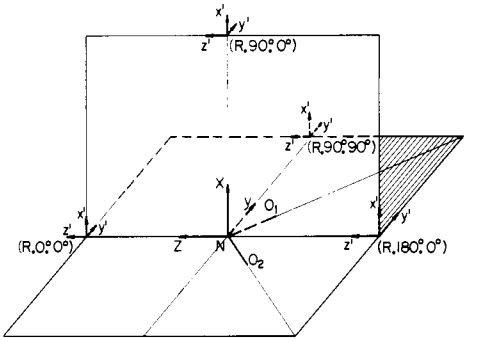

Figure 1. Coordinate system for describing the NO_2^-–H_2O dimer. The NO_2^- is fixed in the yz plane with the coordinate origin at the N atom. (R,θ,Φ) describe the position of the O atom from the H_2O; the angles α, β describe the orientation of its dipole vector and γ shows the rotation angle around the dipole vector.

A. Calculation of the NO_2^-–H_2O Pair Potentials. The NO_2^- basis set employed here (see paper 2 for details) consists of a double-zeta quality contracted Gaussian basis[10] augmented by diffuse s and p functions on the N and O atoms to accommodate the fact that NO_2^- involves a loosely bound "extra" electron. For H_2O, a slightly uncontracted version of the basis of Ditchfield et al.[11] was used. This basis has been shown in paper 2 to give a physically reasonable description of the NO_2^-–H_2O ground-state interaction potential at the SCF level. No counterpoise corrections to computed pair interaction energies have been made in this work.

Because we are not interested here in treating the vibrational contributions to the $n\pi^*$ absorption, we freeze the internal geometry of the NO_2^- ion at its ground-state equilibrium structure.[12] The interaction potential between NO_2^- and H_2O thus involves three coordinates (R,θ,ϕ) (see Figure 1) to describe the relative position of the H_2O molecule and three additional angles (α,β,γ) to describe its orientation.[13] For a balanced description achievement of the energies of the ground- and excited-states of NO_2^-–H_2O, considerable care had to be employed in carrying out these CI calculations. Because the restricted Hartree–Fock (RHF) orbitals of the ground state of the cluster were used to form the CI wave functions of both the ground and excited states, we had to allow for the presence of a large number of singly excited configurations. A set of so-called reference configurations for the ground electronic state was formed by finding those doubly excited configurations (relative to the closed-shell RHF determinant) which interacted strongly (giving an energy lowering relative to the RHF energy of 0.01 au or more). The RHF determinant and this selected group of double excitations then compose the ground-state reference space. The final ground-state CI wave function was then formed by selecting, among all configurations which are either singly or doubly excited relative to these reference determinants, those configurations which caused a ground-state energy lowering of 10^{-6} au or more. To form the excited-state CI wave function, we first performed a CI calculation involving all single excitations relative to the closed-shell ground-state RHF determinant. The appropriate eigenvalue[14] (corresponding to $n\pi^*$

(9) O. Matsuoka, E. Clementi, and M. Yoshimine, *J. Chem. Phys.*, 1351 (1976); G. Bolis and E. Clementi, *J. Am. Chem. Soc.*, **99**, 5550 (1977); R. O. Watts, E. Clement, and J. Fromm, *J. Chem. Phys.*, **61**, 2550 (1974).

(10) T. H. Dunning, *J. Chem. Phys.*, **53**, 2823 (1970).

(11) R. Ditchfield, W. Hehre, and J. A. Pople, *J. Chem. Phys.*, **54**, 724 (1971).

(12) The difference between the equilibrium bond angles (ONO) for NO_2^- and NO_2^-–H_2O was found in ref 8 to be about 0.1. The changes in vibration frequencies, though found to be significantly different for NO_2^- and NO_2^-–H_2O, have minor effects in the structure and excitation energies of the $NO_2^-(H_2O)_n$ cluster.

(13) The orientation of an H_2O molecule relative to the fixed n, y, z axes are defined by rotation angles about an H_2O-body fixed axes x', y', z' which are parallel to the n, y, z axes. The rotations α, β about the y' and x' axes determine the orientation of the dipole vector of H_2O, and γ is the rotation angle around the dipole vector of H_2O.

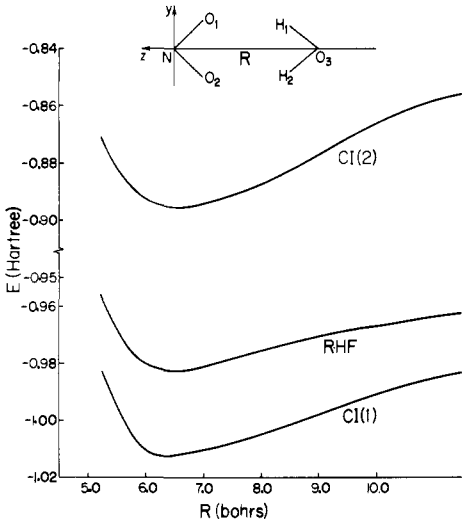

Figure 2. Potential-energy curves for the (R,180,0,0,0,0) conformation of H_2O as a function of R (in bohr). CI(1) and CI(2) refer to the CI energies for the ground and excited electronic states of the dimer.

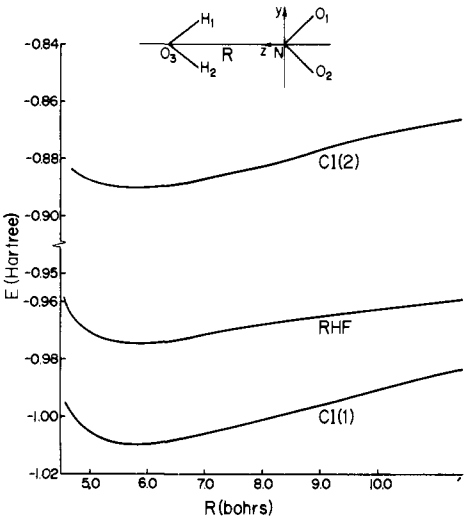

Figure 3. Potential-energy curves for the (R,0,0,180,0,0) conformation of H_2O as a function of R (in bohr). CI(1) and CI(2) refer to the CI energies for the ground and excited electronic states of the dimer.

transition) of this "all singles" CI represents an approximate HF energy for this state because the single excitations allow the ground-state RHF orbitals to relax. Those single excitations, whose expansion coefficients are greater than 0.05, were then used to form a reference space for construction of the final CI wave function. We selected, from among all single and double excitations of the excited-state reference space, those configurations which contributed to the excited-state energy by 10^{-6} au or greater. These configuration selection procedures, which typically involved choosing from approximately 15 000 configurations, thereby lead to what we feel is a relatively balanced description of the ground and excited electronic states. We performed such two-state CI calculations (each of which required approximately 4 CPU h on our DEC 20 computer) at 85 NO_2^-–H_2O geometrical arrangements which were found in oure earlier SCF-level investigation to be most important (populated) at room temperature. The ground- and excited-state potential-energy curves as functions of R are shown for a few typical conformations of the dimer in Figures 2–4.

(14) Certain geometrical conformations of the dimer contain spatial symmetry. For example, if the dimer has C_{2v} symmetry, the $^1A_1$ ground and lowest $^1B_1$ excited state correspond to the two lowest states of separate secular problems. On the other hand, if the dimer has no spatial symmetry, the first excited state corresponds to the second root of a secular problem.

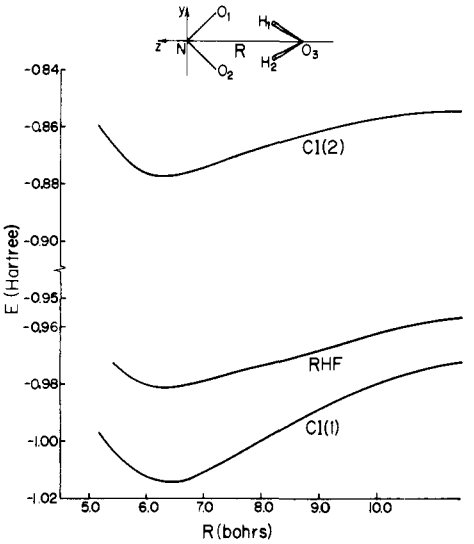

Figure 4. Potential-energy curves for the (R,150,0,320,0,0) conformation of H_2O as a function of R (in bohr). CI(1) and CI(2) refer to the CI energies for the ground and excited electronic states of the dimer.

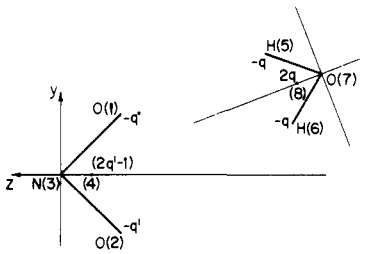

Figure 5. Representaton of the NO_2^- and H_2O molecules used in the model NO_2^-–H_2O interaction potential of eq 3. The indexes (4) and (8) designate the position of the pseudoatoms.

Careful analysis of the results of these CI studies supports much of the findings of our previous work (e.g., the existence of primarily electrostatic interactions, strong tendancy of the OH bonds to orient toward the O or N atoms of NO_2^-, shorter (2.2 Å) O—H··O hydrogen bonds than in neutral systems). There are, however, a few differences in the CI- and SCF-level NO_2^-–H_2O pair potentials which should be pointed out, because they give rise to slightly different predicted structural properties of the $NO_2^-(H_2O)_n$ clusters. First, the minimum-energy N-to-O distance predicted by our CI study (6.0 au) is shorter than that obtained in the SCF study (6.5 au). The CI-predicted lowest energy dimer conformation occurs at conformations described by ($R,\theta,\phi,\alpha,\beta,\gamma$) = (6.0, 150, 0,320,0,0) in contrast to the optimal SCF geometry (6.5, 180, 0,0,0,0). This difference gives rise to differences in the clusters' solvent radial- and angular-distribution function as shown below. Moreover, the CI-level binding energy for the NO_2^-–H_2O dimer (27 kcal/mol) is significantly larger than either the SCF binding energy (17 kcal/mol) or the H_2O–H_2O interaction energy (5 kcal/mol). As is expected, the lowest ($n\pi^*$) state of NO_2^-–(H_2O) is dominated, at all thermally accessible geometries, by configurations involving single excitations of molecular orbitals which are localized on the NO_2^- moiety. The fact that the surrounding solvent molecules are not involved in the excitation event gives substantial support to oure earlier decisions to approximate the excited cluster's solvent pair potentials given in eq 1 and 2 by its ground-state solvent pair potentials (E_{ij}, E_i) and to assume that the nonpairwise additive contributions to the difference in the cluster's ground and excited electronic states can be neglected.

B. Analytical Potential for Dimer Ground and Excited States. To be able to simulate the equilibrium distribution of the conformations of the cluster, we need to have a simple analytical expression for the NO_2^-–H_2O ground- and excited-state pair potentials. We found in paper 2 that the analytical expression of Bernal and Fowler,[15] which is the form used by Clementi for

Table I

parameters	ground state	excited state
q	−2.128804	−5.188833
q'	0.379774	0.126178
a_1	35949.3	95665.2
a_2	5.547442	0.996711
a_3	290.37	245.96
a_4	5.4314	0.507892
b_1	3.014744	2.925567
b_2	1.611081	3.022993
b_3	2.551377	1.817563
b_4	2.027696	2.019020
r_{34}	0.2	0.2
r_{78}	0.487741	0.487741

the H_2O–H_2O pair potential,[9] describes well our RHF-computed energies of NO_2^-–H_2O. In this expression, the short-range repulsion between two atoms i and j is represented in terms of an exponential $a\exp(-b\,r_{ij})$, whereas the long-range attractive potential is expressed as q_iq_j/r_{ij}. Because it seems that both the ground- and excited-state NO_2^-–H_2O interactions are dominated by strong electrostatic interactions, this potential-energy form should be especially relevant. Using this model, we obtain the following expression for the energy of NO_2^-–H_2O relative to the separated fragment species NO_2^- and H_2O (in atomic units with the atomic indices and charges defined in Figure 5.

$$E(NO_2^-\text{–}H_2O) = qq'\left[\left(\frac{1}{r_{15}}+\frac{1}{r_{16}}+\frac{1}{r_{25}}+\frac{1}{r_{26}}\right)+\frac{4}{r_{48}}-2\left(\frac{1}{r_{18}}+\frac{1}{r_{28}}+\frac{1}{r_{45}}+\frac{1}{r_{46}}\right)\right]+q\left[\left(\frac{1}{r_{45}}+\frac{1}{r_{46}}\right)-\frac{2}{r_{48}}\right]+a_1\exp(-b_1r_{37})+a_2[\exp(-b_2r_{15})+\exp(-b_2r_{16})+\exp(-b_2r_{25})+\exp(-b_2r_{26})]+a_3[\exp(-b_3r_{17})+\exp(-b_3r_{27})]+a_4[\exp(-b_4r_{35})+\exp(-b_4r_{36})] \quad (3)$$

The same analytic expression is used for the excited-state surface but with different values for the 10 parameters. Nonlinear least-squares fits of our calculated CI energies to this functional form yielded the two sets of parameters given in Table I. The precision of these fits can be judged by the values of the standard deviations and the sensitivity parameters $\Delta S_K = |p_K\partial\chi/\partial p_K|$, (where p_K designates one of the 10 fitting parameters and χ is the least squares standard deviation). The standard deviations for the ground and excited state were found to be 0.000002 and 0.000006 au, respectively. The stability parameters ΔS_K were used as criteria for stopping the iterative nonlinear least-squares procedure. Convergence was said to be met when all ΔS_K reached 10^{-6} or smaller. As a result, we believe that the above functional form represents our computed NO_2^-–H_2O interaction potentials quite precisely within regions of dimer conformation space which arre likely to be thermally populated at $T = 300$ K. The fact that we seem to be able to determine, with reasonable precision, 8 nonlinear parameters by using only 85 CI-computed energies indicates that the electrostatics-dominated functional form expressed in eq 3 does represent the NO_2^-–H_2O interaction. We expect that had we attempted to use polynomials in $R,\theta,\phi,\alpha,\beta,\gamma$ to "fit" our computed energy values, the resultant fit would not have been nearly as satisfactory. It should also be mentioned that the values of the ground-state potential-surface parameters given in Table I are reasonably close to those which we obtained in paper 2 by fitting our 128 SCF-level NO_2^-–H_2O interaction energies. This fact further supports our belief that we have achieved a physically reasonable fit of our computed energies.

III. Monte-Carlo Simulations of Hydrate Clusters

Once the CI-level potential energy surfaces for the NO_2^-–H_2O dimer have been characterized in an analytical form which is appropriate for the thermally accessible regions of conformation space, we can move on to the Monte-Carlo simulation aspect. As is seen from eq 1, we need to also know the interaction potential between pairs of ground-state water molecules. For this purpose, we have chosen to use the water dimer CI potential surface calculated by Clementi et al.[9] The Monte-Carlo (MC) procedure of Metropolis et al.[16], which we use to study the ground-state equilibrium thermal distribution of various NO_2^-–$(H_2O)_n$ clusters, has been described in detail in paper 2. The ground-state room temperature (T = 300 K) equilibrium distribution of NO_2^-–$(H_2O)_n$ is achieved as follows: (1) An initial conformation (i) is chosen for the n water molecules. For larger cluster sizes, the initial conformation has been taken to be close to the equilibrium-averaged conformation of the cluster having one less H_2O molecule, with an "extra" H_2O placed in an energetically favorable geometry. We did examine the sensitivity of the predicted properties of these larger ($n \gtrsim 10$) clusters to the "starting" position of the nth H_2O molecules. It was found that by allowing the "new" H_2O molecule to be moved by the Monte-Carlo process for an aging period of $\sim 10^4$ passes or moves, it was able to come to equilibrium with the remaining cluster. The resulting equilibrium-averaged properties which are computed did not seem to depend on the starting position of the nth H_2O molecule as long as we allowed the molecule to undergo this aging process. (2) A displacement of one of the water molecules is randomly generated along one of its six geometrical degrees of freedom to give a new conformation (j). This displacement involves changes either in one of the Cartesian coordinates (δ_x, δ_y, or δ_z) of the O atom uniformly distributed on $(-\Delta,\Delta)$ or in an orientational angle α, β, or γ uniformly distributed on $(-\psi,\psi)$. The step lengths Δ and ψ were chosen to give approximately 60% acceptance of the MC passes. (3) The change in the cluster's potential energy ΔE ($= E_j - E_i$) is calculated within the pairwise additive approximation by using our ground-state NO_2^-–H_2O potential function and Clementi's H_2O–H_2O potential function. (4) If the energy change ΔE is negative, the move is accepted; if ΔE is positive, the move is accepted with a probability $\exp(-\Delta E/kT)$ and rejected with probability $[1 - \exp(-\Delta E/kT)]$. The internal geometries of both NO_2^- and H_2O are held fixed, because we are not attempting at this stage to examine vibrational (FC) contributions to the absorption line shape.

Repeated application of these MC steps to the conformational arrangements of the cluster NO_2^-–$(H_2O)_n$ ensures that the sampling of conformations approaches the thermal Boltzmann distribution. An unweighted average of a physical property A taken over t such conformational points q_i approaches the thermal average of A, $\langle A\rangle$, as $t^{-1/2}$

$$\bar{A}_t \equiv (1/t)\sum_i^t A(q_i) = \langle A\rangle + O(t^{-1/2}) \quad (4)$$

More detailed discussion of how the choice of "initial" cluster conformation may effect the fiinal results as well as the "maturing" process used to bring such "initial" distributions close to the thermally probable distributions is given in paper 2. All results reported below involving statistical averages were obtained by averaging over at least 6×10^5 MC passes.

The use of this number of MC passes is justified for two reasons. First, because we begin the MC calculation for a cluster of size n using geometrical information for the cluster of size $n - 1$, it is perhaps more appropriate to consider the *total* number of passes which lead up to those used on the n cluster. On this basis, we have used *more than* 6×10^6 passes rather 6×10^5. Secondly, we observed no appreciable changes in the first, second, and third moments of the excitation-energy distribution (Figure 13) as the number of MC passes was increased beyond 6×10^5. This indicated that the heat capacity of our molecular cluster has also converged. We therefore feel that our computed excitation-energy distribution has converged and 6×10^5 MC passes is indeed adequate when used in the manner outlined above. In point of

(15) J. D. Bernal and F. D. Fowler, *J. Chem. Phys.*, **1**, 515 (1933).

(16) N. Metropolis, A. W. Metropolis, M. N. Rosenbluth, A. H. Teller, and E. Teller, *J. Chem. Phys.*, **21**, 1087 (1953).

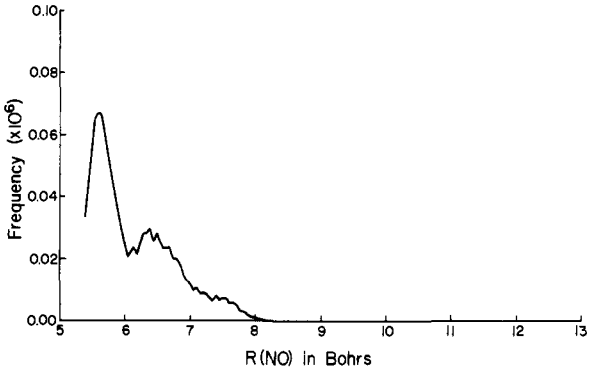

Figure 6. R distribution for $n = 6$.

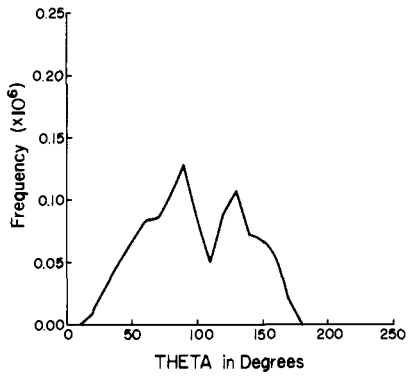

Figure 7. θ distribution for $n = 6$.

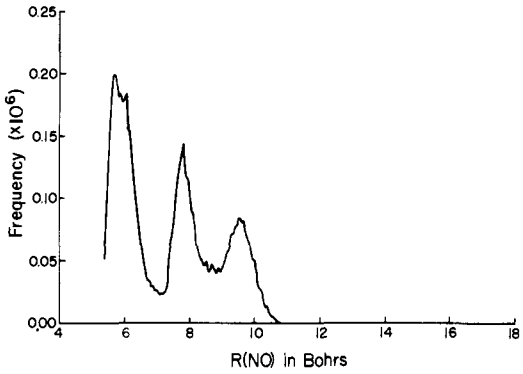

Figure 8. R distribution for $n = 15$.

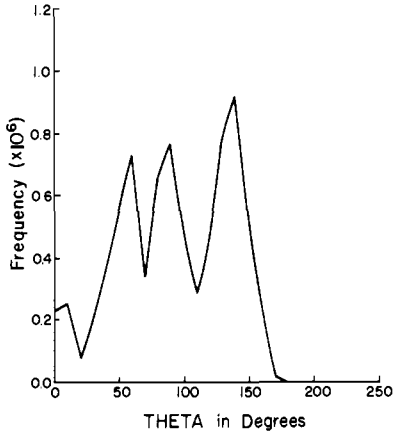

Figure 9. θ distribution for $n = 15$.

fact, we have used more than 10^6 passes for clusters of size 20 and larger.

Although the MC procedure has been widely used in the literature to calculate bulk thermodynamic properties (heat capacities, entropies, etc.), spectroscopic (transition) properties such as excitation energies and their fluctuations have not been frequently examined. At first sight, the evaluation of such transition properties might seem to be beyond the scope of the MC procedure, since these quantities involve both ground- and excited-state interactions with the solvent. However, the electronic transition is a short-time process on the time scale of vibrational, rotational, and translational motion of the cluster. Since we are not interested in following the subsequent fluorescence or decay of the excited ion, we need only simulate the ground-state equilibrium spatial distribution of the cluster. The electronic excitation energy at each conformation is used only to compute the average excitation energy (corresponding to the $0 \rightarrow 0$ vibrational transition) and its fluctuations. The standard MC simulation can thus be straightforwardly applied to evaluate the average excitation energy and its fluctuations as

$$\bar{E}_{ex} = (E_{NO_2^-} - E^0_{NO_2^-}) + \frac{1}{N}\sum_t^N \sum_i^n (E^*_{NO_2^-,i} - E^0_{NO_2^-,i})_t \equiv \frac{1}{N}\sum_t^N E_{ex,t} \quad (5)$$

$$\sigma_2^2 = \langle (E_{ex} - \bar{E}_{ex})^2 \rangle = \frac{1}{N}\sum_t^N (E_{ex,t} - \bar{E}_{ex})^2 \quad (6)$$

and

$$\sigma_3^3 = \langle (E_{ex} - \bar{E}_{ex})^3 \rangle = \frac{1}{N}\sum_t^N (E_{ex,t} - \bar{E}_{ex})^3 \quad (7)$$

The average excitation energy of the aqueous NO_2^- (aq) system can be simulated by progressively increasing the cluster size n until this property ($\bar{E}_{ex}$) stabilizes, i.e., until further increase in n does not alter $\bar{E}_{ex}$. This procedure should converge because the electron which is excited is highly localized on the nitrite ion.

As a byproduct of the MC studies we also gain valuable information about the shapes of these small clusters as expressed in terms of the positions (R,θ,Φ) of the water molecules around the NO_2^- ion. Because we have already reported such results in paper 2 where we used the RHF-level NO_2^-–H_2O pair potential, we shall only briefly outline the highlights of some of our present findings (using the CI NO_2^-–H_2O potential) relating to the cluster structures.

For clusters involving five or few water molecules, we find the formation of part of the first hydration layer to involve water molecules distributed in the $\theta > 90°$ hemisphere. For the six-water cluster, whose radial and angular distribution functions are shown in Figures 6 and 7, we find substantial probability of finding the sixth H_2O near $R \simeq 7$ au and $\theta > 90°$. This hints that the second hydration layer seems to begin to form behind the incomplete first layer before the $\theta < 90°$ component of the first hydration shell is filled.[19] This unusual result is not an artifact of where we placed the sixth H_2O molecule to begin the MC simulation. We found that even when the sixth H_2O molecule was put into the $\theta < 90°$ region close to the N atom of the NO_2^-, it moved during the MC process to the $\theta > 90°$ region. This somewhat surprising behavior of the $n = 6$ cluster can be interpreted in terms of the anisotropy of the NO_2^-–H_2O pair potential and the relative strengths of the NO_2^-–H_2O (27 kcal/mol) and H_2O–H_2O interactions (5 kcal/mol). The tendency of the sixth water molecule to reside near $R \sim 7$ au (i.e., in the second hydration layer) with $\theta > 90°$ is due to a local cooperative effect involving the first five water molecules which cause the $\theta < 90°$ hemisphere to be less attractive to an "incoming" sixth water because of the repulsive dipole–dipole interactions they present to an approaching sixth water.

The features which characterize the $(n > 6)$ clusters can be summarized as follows:

(i) As successively more H_2O molecules are added, they fill both the $\theta < 90°$ part of the inner hydration shell as well as the second hydration shell (again, the $\theta > 90°$ portion is filled first). As n grows, the water molecules present in the inner hydration shell increasingly populate the $\theta < 90°$ regions.

(ii) The anisotropy of the NO_2^-–H_2O potential is further manifested in the existence of a pronounced third hydration layer near $R \simeq 10$ au as is illustrated in Figure 8 for the radial distribution of the 15 water cluster.

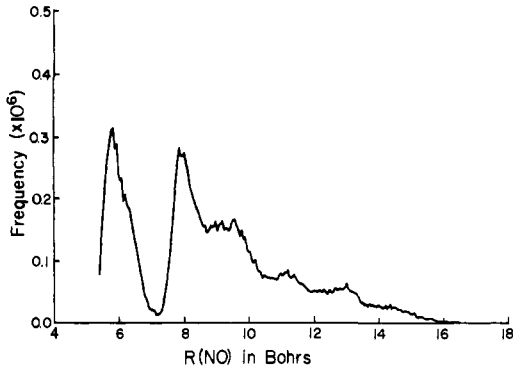

Figure 10. R distribution for $n = 25$.

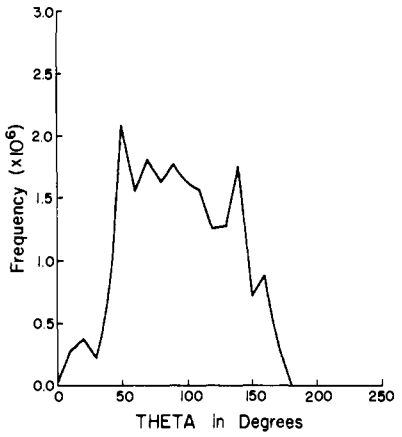

Figure 11. θ distribution for $n = 25$.

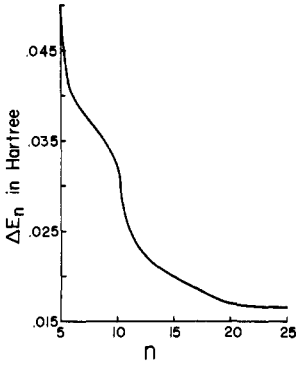

Figure 12. Behavior of total ground-state energy differences $\overline{\Delta E_n} = \bar{E}_n - \bar{E}_{n+1}$ (hartree) as a function of the cluster size, n.

(iii) Once n has reached 15, the θ distribution (Figure 9) shows that the NO_2^- ion is surrounded by at least one complete layer of water molecules. The fact that the θ distribution for $n = 15$ displays significant structure indicates that the strong NO_2^-–H_2O interaction has a substantial influence on even the 15 H_2O molecule. The R and θ distributions for $n = 25$ (Figures 10 and 11) show that the outer H_2O molecules residing in the $10 < R < 16$ au range are comparatively loosely bound.

To examine the trend in the hydration energies as a function of the cluster size n, we show in Figure 12 the differential energy increment $\Delta E_n^0 = \bar{E}_n^0 - \bar{E}_{n+1}^0$ for $5 \leq n \leq 25$. Since ΔE_n^0 corresponds to the energy required to remove the $(n+1)^{st}$ water molecule from the NO_2^-–$(H_2O)_n$ core, it should tend, for large n [where our results are assumed to simulate the NO_2^- (aq)], to a constant value. As Figure 12 shows by $n \simeq 25$ a stable value of ΔE_n^0 is indeed obtained. Castleman et al.[5] and Kebarle et al.[6] have measured the differential enthalpy change ΔH_n° ($= H_n^\circ - H_{n+1}^\circ$) for small NO_2^-–$(H_2O)_n$ clusters for $n = 1,2,3$. In paper II we performed similar MC simulations on small NO_2^-–$(H_2O)_n$ clusters, by using our SCF-level NO_2^-–H_2O dimer potential. The resultant ΔE_n^0 vs. n curve which is shown in paper 2 is found to be remarkably parallel to the experimental ΔH_n° curve of Castleman et al. Thus, it might be expected that our predicted differential energies of hydration for larger ($n \geq 3$) clusters could be reasonably reliable.

Table II. Distribution of $n\pi^*$ Excitation Energies and Their Fluctuations

n	6	15	20	25
$\bar{E}_{ex}$, eV	3.11	3.08	3.08	3.07
σ_2, cm^{-1}	812	809	808	808
σ_3, cm^{-1}	342	200	176	210

The main differences in the structure of clusters as predicted by using the CI- and SCF-level description of the interaction potentials are that (i) the water molecules in the CI description are packed closer to the NO_2^- ion, as seen by the radii of the first hydration layers ($R \simeq 5.8$ au for the CI potential and $R \simeq 6.8$ au for the RHF potential) and (ii) the water molecules as described by the CI potential have smaller flexibility of movement in the radial and angular degrees of freedom as reflected in the narrower peaks of the R distribution and in the structure displayed the θ distribution even for $n = 6$. These observations can be understood in terms of the differences in the CI- and RHF-potential surfaces discussed in section III. The lowest energy conformations of the CI surface lie in the range of $90° \leq \theta \leq 150°$ at $R = 6.0$ au, whereas the RHF surface has its low-energy regions near $R = 6.5$ au and $\theta = 180°$. The rigidity of the water molecules around the nitrite ion is due to the fact that the CI surface is generally "deeper" and has a much larger binding energy than the RHF surface.

Distribution of Electronic Transition Energies. Given the insight that the structures of the above discussed clusters have given us, we can now move on to discuss the results of our MC simulation of the $n\pi^*$ transition energy and its fluctuations. As we discussed earlier, MC simulations were performed for progressively larger clusters until the equilibrium averages of these quantities are unchanged.

To emphasize how various fluctuations in the electronic excitation energy contribute to the spectral line shape, we recall from paper 1 that the Fourier transform of the electric dipole correlation function involves inhomogeneous broadening of each vibrational line caused by fluctuations in the solvent molecules' instantaneous positions. In the theory of optical absorption spectra developed by us in paper 1, Kubo's cumulant expansion technique was employed within a short-time approximation to write the time dependence of the electric dipole correlation function (CF) as

$$\mathrm{CF} = \exp\left[-\frac{i}{\hbar}\bar{E}_{ex}t - \left(\frac{1}{2!}\right)\left(\frac{\sigma_2^2}{\hbar^2}\right)t^2 + \left(\frac{i}{3!}\right)\left(\frac{\sigma_3^3}{\hbar^3}\right)t^3 \ldots\right] \quad (8)$$

where σ_2^2 and σ_3^3 are the quadratic and cubic fluctions in the excitation energy given in eq 6 and 7. The Fourier transform of the first term in eq 8 gives a "δ-function" spectrum, whereas the inclusion of the second term yields a Gaussian broadening of each of the vibrational lines. The cubic and higher order fluctuation terms have been neglected in most treatments of bulk equilibrium statistical mechanical properties. In our present MC calculations, the results of which we describe below, we calculated these cubic fluctuations for various cluster sizes. This study hence provides us with a unique opportunity to examine how significant these cubic fluctuations are in determining the spectral line shape.

Table II shows the equilibrium averaged values of the excitation energy as well as the quadratic and cubic fluctuations as functions of the cluster size. It should be noted that for $n = 25$, all of these transition properties have become quite stable and hence may be used to approximate the NO_2^- (aq) values. As should be apparent from the R and θ distributions for $n = 6$ shown in Figures 6 and 7 and the potential surfaces shown in Figures 2–4, the excitation energy and fluctuations would not be expected to be stable for such small cluster sizes; the completion of the hydration layers which have significant effects on the distribution of NO_2^- electronic excitation energies is not achieved until $n > 20$. Figure 13 shows

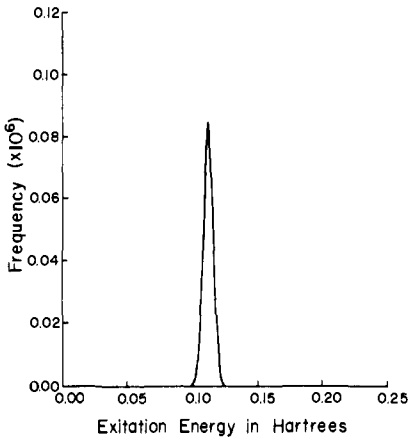

Figure 13. $n\pi^*$ excitation ($0 \rightarrow 0$) energy distribution for $n = 25$.

the distribution of the $n\pi^*$ excitation energy for $n = 25$.

The "large n" value of the average excitation energy corresponding to the $0 \rightarrow 0$ vibrational transition (band origin) is found to be 3.07 eV, which is in very close agreement with the value of 3.08 eV found in ref 8 by fitting the experimental spectrum with our line shape model. Comparing this value to the gas-phase (theoretical) value of 3.5 eV obtained in our CI study or the value of 3.2 eV arising in the experimental probe of $NaNO_2$ crystal,[17] one finds that hydration has produced significant differential stabilization ($\sim$0.43 eV) of the excited state relative to the ground state. Similar large "solvation" effects have also been observed[17] in crystals containing NO_2^- and larger cations (Cs^+ or K^+).

The inhomogeneous broadening (the square root of the quadratic fluctuation of the excitation energy) is found from Table II to be 808 cm^{-1} which is about a factor of 2 larger than the 400-cm^{-1} value of σ^2 obtained by applying our earlier[8] model to the experimental spectrum. This discrepancy then supports our earlier claim[8] that the "fitting" procedure put forth in ref 8 and discussed in ref 2c usually leads to inhomogeneous broadening factors which are lower bounds to the true values. Unfortunately there is no directly measured value of σ for NO_2^- with which we can compare our two estimated values. The cubic fluctuation of the excitation energy, which is found here to be 210 cm^{-1}, would have the effect of skewing the otherwise Gaussian shape of the inhomogeneously broaded vibrational absorption lines. At first sight, the magnitude of this value (210 cm^{-1}) when compared to the value of σ_2 (810 cm^{-1}) may be surprising. In our earlier development, and in most statistical mechanical treatments of equilibrium properties, the effects of cubic (and higher) fluctuation have been neglected. It seems that such may not be a valid assumption for the present case. However, a stationary-phase analysis[18] of the Fourier transform of eq 9 shows that these cubic fluctuations σ_3 contribute to the absorption intensity relative to the contributions of quadratic fluctuations σ_2 in a ratio of $2\text{-}(\sigma_3^3/3)\sigma_2^3$. Using our values of σ_2 and σ_3, this ratio is equal to 1/50. Although this analysis shows that the effects of cubic fluctuations may be small for the hydrated nitrite ion's electronic spectrum, recent development is picosecond spectroscopy may enable one to observe these higher order effects by examining spectra within the time domain rather than in frequency space.

IV. Summary

We have carried out a Monte-Carlo simulation of the solvation structure and $n\pi^*$ electronic absorption line shape (for the $0 \rightarrow 0$ transition) of the aqueous nitrite ion by examining successively larger $NO_2^-(H_2O)_n$ clusters. We found the structure of these clusters to be dominated by the strong (27 kcal/mol) anisotropic NO_2^-–H_2O pair potential which preferentially locates the first several H_2O solvent molecules in the $\theta > 90$s hemisphere. Energetically favorable conformations of the inner hydration shell were found to lie in an annulus of $5.8 \leq R \leq 6.5$ au with the H atoms of the water molecules aligned toward either the N atoms or the O atoms of NO_2^-. We found that (for $n = 6$) for the first or inner hydration shell does not necessarily fill before the second layer begins to form. This result, which is due to the anisotropic nature of the NO_2^-–H_2O interaction and the local cooperative interactions among the H_2O solvent molecules, should, as mentioned by Clementi et al.,[19] caution other workers who attempt to simulate hydration-shell structures of such systems.

For the $n\pi^*$ electronic excitation of the aqueous nitrite ion, the calculated ($0 \rightarrow 0$) excitation energy and its quadratic fluctuation are found to be reasonably well reproduced by the MC simulations, although the inhomogeneous broadening differs by a factor of 2 when compared to the value we previously obtained by fitting the experimental spectrum to our earlier model. We also found that the effects of cubic fluctuations in the excitation-energy distribution may not be entirely negligible.

Acknowledgment. This research was supported by the National Science Foundation through Grant 7906645. Most of the calculations presented here were performed on the University of Utah's DEC 20/60 computer which was partially funded by the National Science Foundation.

(17) J. W. Sidman, *J. Am. Chem. Soc.*, **79**, 2669 (1957); **79**, 2675 (1957).

(18) J. Mathews and R. L. Walker, "Mathematical Methods of Physics", W. A. Benjamin, New York, 1970.

(19) E. Clementi and R. Ranghino, *Gazz. Chim. Ital.*, **108**, 157 (1978).